JOURNAL OF GEOPHYSICAL RESEARCH, VOL. 107, NO. A6, 1086, 10.1029/2001JA900153, 2002

Substorm energy budget during low and high solar activity: 1997 and 1999 compared

E. Tanskanen, T. I. Pulkkinen, and H. E. J. Koskinen[1]
Finnish Meteorological Institute, Helsinki, Finland

J. A. Slavin
NASA Goddard Space Flight Center, Greenbelt, Maryland, USA

Received 12 April 2001; revised 18 September 2001; accepted 18 September 2001; published 26 June 2002.

[1] Substorms during the years 1997 and 1999 are analyzed to examine substorm energy budget just after solar minimum and prior to solar maximum. The energy input from the solar wind into the magnetosphere is estimated in terms of the time integral of Akasofu's epsilon parameter computed from Wind and ACE observations. The ionospheric Joule heating dissipation is estimated using the local electrojet index *IL* derived from the IMAGE magnetometer array of the MIRACLE ground-based network in the Scandinavian sector. In total, 839 substorms from the midnight sector have been investigated to show that on average the Northern Hemisphere Joule heating accounts for ~30% of solar wind energy input during 1997 and 1999 substorms. We found that during the active year 1999, there were 26% more substorm events, they were 15% more intense, and they were located at lower latitudes than during 1997. Isolated and stormtime substorms were also examined separately. Mean intensity of isolated substorms was about −350 nT, whereas it was about −670 nT for stormtime events. This study confirms our previous results (for 1997 only) that the amount of Joule dissipation depends on the energy input during the substorm expansion phase. Furthermore, the correlation is best for substorms recorded in the postmidnight sector, indicating that the energy budget and substorms size are largely controlled by processes driven directly by the solar wind. *INDEX TERMS:* 2788 Magnetospheric Physics: Storms and substorms; 2437 Ionosphere: Ionospheric dynamics; 2784 Magnetospheric Physics: Solar wind/magnetosphere interactions; 2736 Magnetospheric Physics: Magnetosphere/ionosphere interactions; *KEYWORDS:* substorms, energetics, Joule heating

1. Introduction

[2] Growing interest in space weather activities during the past few years has made global magnetospheric energy budget studies increasingly important. Several single-event studies have been made to define the role of different dissipation channels in the global energy budget [e.g., *Akasofu*, 1981; *Pulkkinen et al.*, 2002]. However, there are hardly any quantitative studies on the relative importance of the different dissipation channels, even though the essential tools and approximative empirical formulas for large statistical energy budget studies have been available for some time [e.g., *Akasofu*, 1981; *Ahn et al.*, 1983; *Weiss et al.*, 1992].

[3] The global energy flow from the Sun is transported via the solar wind to the Earth. Different interplanetary coupling functions have been used to estimate the energy entering the Earth's magnetosphere. Many of them exhibit various characteristics of the solar wind-magnetosphere interaction, and choosing one over another depends on the purpose of the study [e.g., *Holzer and Slavin*, 1982; *Stamper et al.*, 1999]. The epsilon parameter [*Perreault and Akasofu*, 1978; *Akasofu*, 1981] has been one of the most popular means to measure the energy input.

[4] Understanding the dynamics of magnetospheric substorms is essential for the study of the global energy budget. Substorms are transient processes during which a significant amount of energy derived from the solar wind magnetosphere interaction is deposited in the auroral ionosphere, in the ring current encircling the Earth, in the plasmoid formation, and in the plasma sheet heating in the Earth's magnetotail [e.g., *Weiss et al.*, 1992; *Ieda et al.*, 1998]. For a long time the ring current was thought to be the main dissipation channel of magnetospheric energy [*Akasofu*, 1981]. However, the results of recent studies have indicated that Joule heating dominates over the other dissipation channels during disturbed periods [e.g., *Lu et al.*, 1995; N. E. Turner et al., Global energy partitioning during magnetic storms, submitted to *Journal of Geophyical Research*, 2001, hereinafter referred to as Turner et al., submitted manuscript, 2001]. It must, nevertheless, be remembered that most of the earlier studies concentrated on storms, and it is not clear whether these results hold true for substorms.

[1]Also at Department of Physics, University of Helsinki, Helsinki, Finland.

0148-0227/02/2001JA900153$09.00

[5] Auroral electrojet indices, *AE*, *AU*, and *AL* [*Davis and Sugiura*, 1966], have been widely employed in estimating the amount of solar wind energy dissipated in the magnetosphere and in the ionosphere [e.g., *Bargatze et al.*, 1985; *Petrukovich et al.*, 2000]. As the latitudinal coverage of the *AE* magnetometers is not sufficient for auroral electrojets located at very high or very low latitudes, indices derived from a well-situated roughly longitudinal magnetometer chain represent the real ionospheric activity better. *CU*/*CL* indices from the CANOPUS chain [*Rostoker et al.*, 1995] and the *IU*/*IL* indices from the IMAGE chain [*Kallio et al.*, 2000] are examples of such indices. According to *Kauristie et al.* [1996] the maximum electrojet activity derived from the IMAGE chain represents the ionospheric activity as well as, or better than, the *AE* index within the local time sector from 1500 to 0130 UT.

[6] Substorms can be divided into isolated and stormtime substorms [*Baumjohann et al.*, 1996; *Kamide et al.*, 1998]. Recently, it has been discussed whether stormtime substorms differ from their isolated counterparts, and if so, what the main differences would be. *Baumjohann et al.* [1996] suggest that there may be fundamental differences between these two subclasses of substorms. They also speculate that substorms may be caused by two different mechanisms: near-Earth reconnection for the stormtime substorms [e.g., *McPherron et al.*, 1973; *Hones et al.*, 1984] and current disruption for the isolated substorms [e.g., *Lu et al.*, 1998]. The opposite view is that there is no qualitative difference between isolated and stormtime substorms [e.g., *Hsu and McPherron*, 2000].

[7] In our previous paper [*Kallio et al.*, 2000] we examined the loading-unloading processes during magnetospheric substorms that occurred in 1997 by examining all substorms in the time sector between 1600 and 0200 UT, where the *IL* index reached at least −100 nT. We concluded that the strongest correlation, 0.71, between the integrated energy input from the solar wind and the integrated energy dissipated in the ionosphere was given by the energy input to the system after the substorm onset. Hence, while the energy loaded into the magnetotail during the growth phase is needed for the magnetospheric reconfiguration before the substorm onset, the size of the substorm is mostly governed by the direct energy input during the expansion phase.

[8] This study continues our earlier work by analyzing both isolated and stormtime substorms during two years, 1997 and 1999. The aims of this paper are to respond to the need for extensive statistical studies by examining the energy budgets of more than 800 substorms, compare isolated and stormtime substorms, and look for the differences between the different solar cycle phases. Each event has been characterized by using the following parameters: duration, time of onset, maximum intensity, onset latitude, amount of energy input, and Joule heating dissipation. As measures of total energy input and Joule dissipation, we use time integrals of the epsilon parameter and the *IL* index over complete substorm cycles. Similar integrals have been successfully used to investigate magnetic energy flux into and out of the tail lobes by *Holzer and Slavin* [1981] and *Moldwin and Hughes* [1993], and to investigate the energy budget of storms [*Pulkkinen et al.*, 2002] and substorms [*Petrukovich et al.*, 2000].

Table 1. Sites and Coordinates of 16 IMAGE Array Stations

IMAGE Station	Geographic Coordinates		Year
	ϕ, °N	λ, °E	
NAL Ny Ålesund	78.92	11.95	97, 99
LYR Longyearbyen	78.20	15.82	97, 99
HOR Hornsund	77.00	15.60	97, 99
HOP Hopen Island	76.51	25.01	97, 99
BJN Bear Island	74.50	19.20	97, 99
SOR Sørøya	70.54	22.22	97, 99
KEV Kevo	70.54	27.10	97, 99
TRO Tromsa	69.76	18.94	97, 99
MAS Masi	69.46	23.70	97, 99
AND Andenes	69.30	16.03	99
KIL Kilpisjarvi	69.02	20.79	97, 99
ABK Abisko	68.35	18.82	99
MUO Muonio	68.02	23.53	97, 99
LOZ Lovozero	67.97	35.08	99
KIR Kiruna	67.84	20.42	99
SOD Sodankylä	67.37	26.63	97, 99
PEL Pello	66.90	24.08	97, 99
LYC Lycksele	64.61	18.75	99
OUJ Oulujärvi	64.52	27.23	97, 99
HAN Hankasalmi	62.30	26.65	97, 99
NUR Nurmijärvi	60.50	24.65	97, 99
UPS Uppsala	59.90	17.35	99

[9] The purpose of this paper is to examine the relative role of Joule heating in the global magnetospheric energy budget during periods near solar minimum and rising solar activity. Furthermore, we report on statistical results about the intensities and onset latitudes of substorms. In section 2 we illustrate our database. The characterization of the substorms (duration, intensity, and latitude) is presented in section 3. In section 4 we analyze isolated and stormtime substorms separately and look for the differences between these two subclasses. In section 5 we finally provide for a comparison of substorms occurring during low (1997) and high solar activity (1999), and section 6 concludes with discussion.

2. Data Set

[10] In this paper a substorm is defined as an interval of increased energy dissipation to the auroral ionosphere, which is determined from the westward auroral electrojet index [*Kallio et al.*, 2000]. This definition is consistent with the operational definition of substorms recommended by *Rostoker et al.* [1980]. The proxy of the westward electrojet index AL, which we call the IL index is constructed from 16 (22) magnetometers of the IMAGE array of the MIRACLE ground-based network for 1997 (1999) (see Table 1) [*Syrjäsuo et al.*, 1998]. All substorms, with intensity larger than −100 nT, and occurring between 1600 and 0200 UT were selected to the database, because during this UT interval the IMAGE is near the local midnight and gives a good estimate of the standard AL index [*Kauristie et al.*, 1996].

[11] The threshold of −100 nT is, of course, an arbitrary choice. There is no unique minimum level of electrojet activity that would qualify as a substorm. Stronger activity often does not represent a substorm and, on the other hand, one can argue that small substorms do not need to reach −100 nT. However, including too weak events would introduce too many unclear cases in the database. Thus substorm in the present study means a substorm reaching

at least −100 nT in the *IL* index. Note that many of these events would be weaker than −100 nT using the *AE* index. As will be shown later, the maximum electrojet of weak isolated substorms is often located north of the standard *AE* station Abisko. A further requirement was a clear onset of activity, which distinguished small substorms from generally more disturbed periods.

[12] The full data set examined here, 839 substorm events, covers the period from 1 January 1997 to 31 December 1997 and from 1 January 1999 to 30 November 1999. The used IMAGE magnetic records have a 60-s resolution averaged from the original 10-s data. The solar wind and interplanetary magnetic field data were obtained from the Wind and ACE satellites. Data from the Wind magnetic field instrument (MFI, at 60-s resolution) [*Lepping et al.*, 1995] and Solar Wind Experiment (SWE, at 92-s resolution) [*Ogilvie et al.*, 1995] were used during 1997, and the ACE Magnetic Field Experiment (MAG, at 16-s resolution) [*Smith et al.*, 1998] and solar wind electron proton alpha monitor (SWEPAM, at 64-s resolution) [*McComas et al.*, 1998] were used for 1999. Over 58% of the investigated events took place during the more active year 1999.

[13] The energy input from the Sun via the solar wind to the magnetosphere is estimated by computing Akasofu's epsilon parameter from the Wind and ACE spacecraft magnetic field and solar wind measurements. The epsilon parameter is given in SI units as

$$\epsilon(\mathrm{W}) = 10^7 \cdot V(\mathrm{m/s}) B^2(\mathrm{T}) \sin^4(\theta/2) \cdot l_0^2(\mathrm{m}), \qquad (1)$$

where V is the upstream solar wind speed, B the interplanetary magnetic field (IMF) intensity, θ the IMF clock angle ($\tan\theta = B_y/B_z$) in geocentric solar magnetospheric (GSM) coordinates, and l_0 an empirical parameter to fit energy input to the total estimated output. Following *Perreault and Akasofu* [1978] and *Akasofu* [1981], the value l_0 is taken as 7 R_E. In the present study we compute the time integral of energy input, $W_\epsilon = \int \epsilon\, dt$, from the beginning of the growth phase to the end of the recovery phase. We have shifted the solar wind time series to account for the time delays from Wind and ACE to the coupling region ($X(GSM) = 10\ R_E$) by $\Delta t = \Delta X/V$, where V is the average speed observed around the substorm onset time.

[14] It is generally accepted that the Z component of IMF controls the energy input to the magnetosphere. The substorm sequence begins when a southward turning of the IMF activates dayside reconnection [*Baker et al.*, 1984; *Baker*, 1996; *Russell and McPherron*, 1973]. The entire polar ionosphere responds normally within 2 min [*Ridley et al.*, 1997, 1998; *Ruohoniemi and Greenwald*, 1998] or at latest, after 15 min [*Cowley and Lockwood*, 1992] to the new IMF conditions at the magnetopause.

[15] In the present study the substorm was first identified from the IMAGE data. The beginning of the substorm growth phase was determined from the moment of the *IMF* southward turning. While the determination of the exact starting point of integration is not always unique, possible errors introduced to the integrated energy input remain small owing to the strong dependence of the epsilon parameter on the southward IMF. The event is considered to end when the *IL* index returns back to the quiet level values after the recovery phase. In the present study the expansion phase onset is determined from the *IL* index, when it shows a rapid decrease that leads to a negative bay development.

[16] For input-output analysis we could simply look for correlation between integrated epsilon (J) and integrated *IL* (nT · s). However, as we are ultimately interested in quantitative energy budget, the *IL* index is converted to Northern Hemisphere Joule heating by the empirical formula $P(\mathrm{W}) = 3 \cdot 10^8 IL$ (nT) following *Ahn et al.* [1983]. As discussed by *Lu et al.* [1998], various attempts to relate the Joule heating rate to the *AE* index have given results varying from 0.21 to 0.54 GW/nT. *Lu et al.* [1998] used the assimilated mapping of ionospheric electrodynamics (AMIE) technique to model the January 1997 storm using *AE* calculated from 68 magnetometer stations and found the relation to be at the lower end of this interval. On the basis of these results together with the previously mentioned fact that *IL* gives a good representation of *AL* in the investigated time sector the proportionality factor 0.3 GW/nT to convert *IL* to Joule heating is used in the present statistical study. Finally, the Joule dissipation energy W_{IL} is calculated as $W_{IL} = \int P(\mathrm{W})dt$ either over the same time period as the epsilon is integrated.

2.1. First Example: 23 June 1997

[17] Figure 1a displays 8 hours of simultaneous, 60-s averaged solar wind and ground-based measurements on 23 June 1997. The event was a medium-sized isolated substorm reaching its maximum intensity −300 nT in Tromsø magnetometer station (geographic latitude 69.76°, geographic longitude 18.94°). Solar wind energy input started at 2044 UT when the IMF B_z turned rapidly southward, from +5 to −5 nT. Soon after that, the epsilon power reached almost 4×10^{11} W. At 2205 UT a substorm onset took place leading to the substorm expansion, followed by another, much larger, intensification half an hour later. At the same time with the IMF B_z northward turning, the epsilon power returned from the maximum to quiet level values resulting in 1.3×10^{15} J total energy input over the period of southward IMF and substorm activity. Total hemispheric Joule dissipation over the same period was 0.35×10^{15} J, ∼27% of the input.

2.2. Second Example: 1 March 1999

[18] An intense, stormtime substorm occurring during the storm recovery phase (*Dst* about −60 nT) was observed on 1 March 1999 (Figure 1b). Minimum value of the *IL* index, −871 nT, was measured at the Kevo magnetometer station (geographic latitude 70.54°, geographic longitude 27.10°). Solar wind energy input started at 2323 UT. The IMF B_z turned from +4 to −12 nT in several steps during a period of 1.5 hours. Energy input continued 2.5 hours resulting in 7.9×10^{15} J total energy input. Ionospheric Joule dissipation started at 2350 UT growing gradually, without any clear intensifications related to the stepwise evolution of the energy input. The hemispheric Joule dissipation was 1.9×10^{15} J, i.e., ∼24% of energy input.

3. Substorm Properties

[19] In this section we introduce the classification of the different substorms in our study and discuss the duration, intensity, and latitudinal distribution of the events that all bear significance to the interpretation of the results of this study.

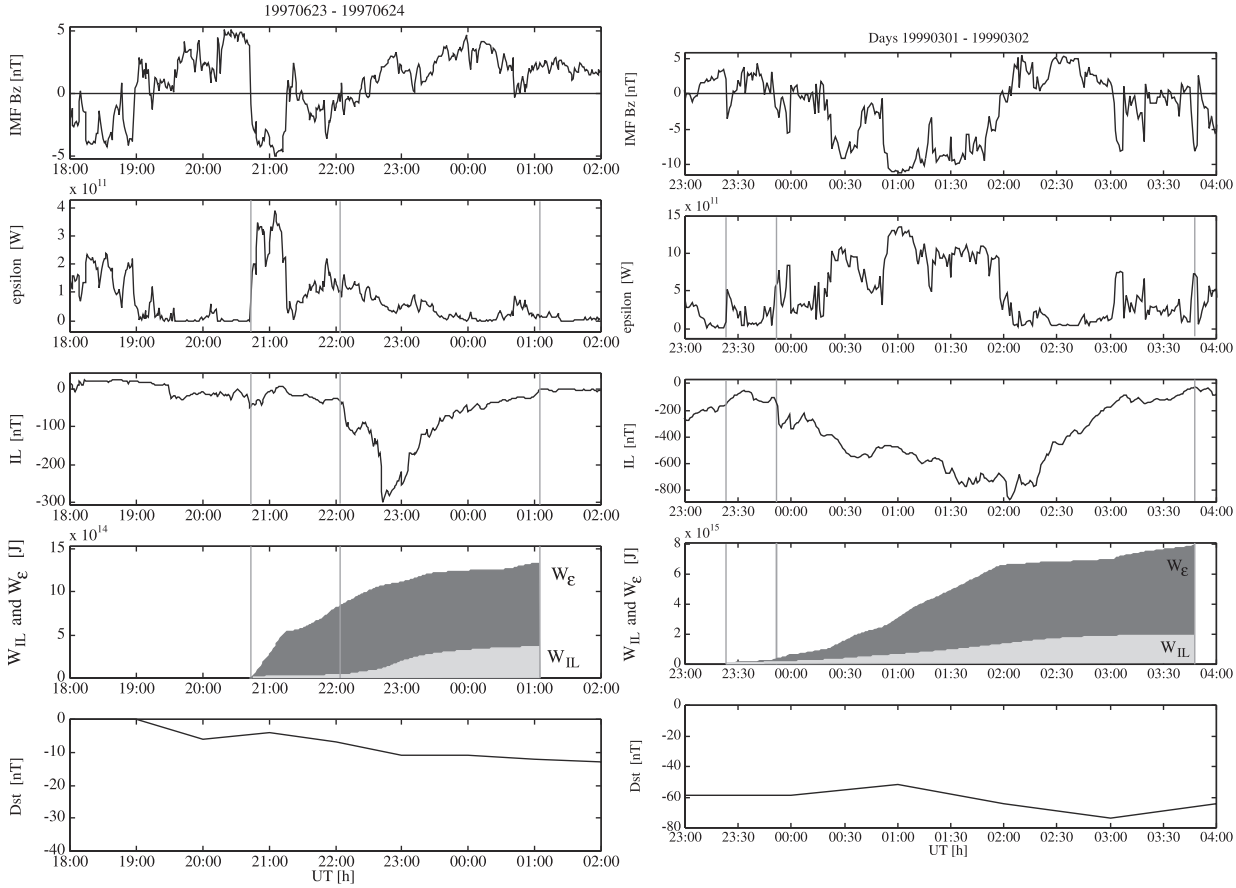

Figure 1. (a) Isolated substorm on 23 June 1999. The maximum intensity was recorded at 2240 UT in Tromsø (geographic latitude 69.76°). (b) Stormtime substorm on 1 March 1999. The maximum intensity took place at Kevo (geographic latitude 70.54°). Panels from top to bottom: IMF B_z, ϵ, *IL* index, W_ϵ, and W_{IL}.

3.1. Substorm Classes

[20] We classify substorms to various groups in the following ways: (1) events during the year of low solar activity (1997) versus events during the year of high solar activity (1999); (2) isolated versus stormtime substorms; and (3) premidnight versus postmidnight substorms (Figure 2). The more active year substorms account for over half of events in the database: there were 405 isolated events and 82 stormtime events within the investigated local time sector in 1999. In 1997 the corresponding numbers were 293 and 59, thus isolated substorms account for a vast majority of all events. Substorms were identified as isolated when the *Dst* index during the event did not reach the limit for minor storms, which we put in this study to −40 nT. The events were classified as two separate events if there were ∼2 hours between the end of the first intensification and the start of the next intensification. Events with substorm onset (the time of the start of the expansion phase) before 2130 UT, which is the local midnight in the time sector of the IMAGE magnetometers, were classified as premidnight events, others were categorized as postmidnight events. Figure 2a illustrates the solar activity by the sunspot number in years 1995–2001, highlighting the low-activity year 1997 and the more active year 1999. Figure 2b shows the number of events in each of the categories.

3.2. Substorm Duration

[21] As discussed in section 2, the beginning of the substorm growth phase is determined from the IMF southward turning, while the substorm onset and the end of substorm are both determined from the *IL* index. The end of the substorm is more difficult to determine than the onset: In our analysis the endpoint was determined from the return of the *IL* index to the magnetically quiet level. Because the IMAGE magnetometers do not record night-sector activity adequately beyond 0200 UT [*Kauristie et al.*, 1996], the magnetometers being already 4.5 hours past the local midnight, some events that continued further than 0200 UT seemed shorter than they would have been if a latitudinal network had been used. The onsets of the substorms form a single-peaked, nearly Gaussian distribution over the time period 1600–0200 UT with a mean onset time at 2023 UT (∼2250 MLT).

[22] The mean duration of all studied substorms was 3 hours 48 min, the mean duration being 3 hours 42 min for premidnight substorms and 4 hours 6 min for postmidnight substorms. As some of the postmidnight events were cut at 0200 UT, the latter value is slightly underestimated (Figure 3). This difference in durations most probably is due to the fact that when the chain is in the morning sector, it records better the sustained morning-sector westward electrojet activity that often occurs during the substorm recovery phase.

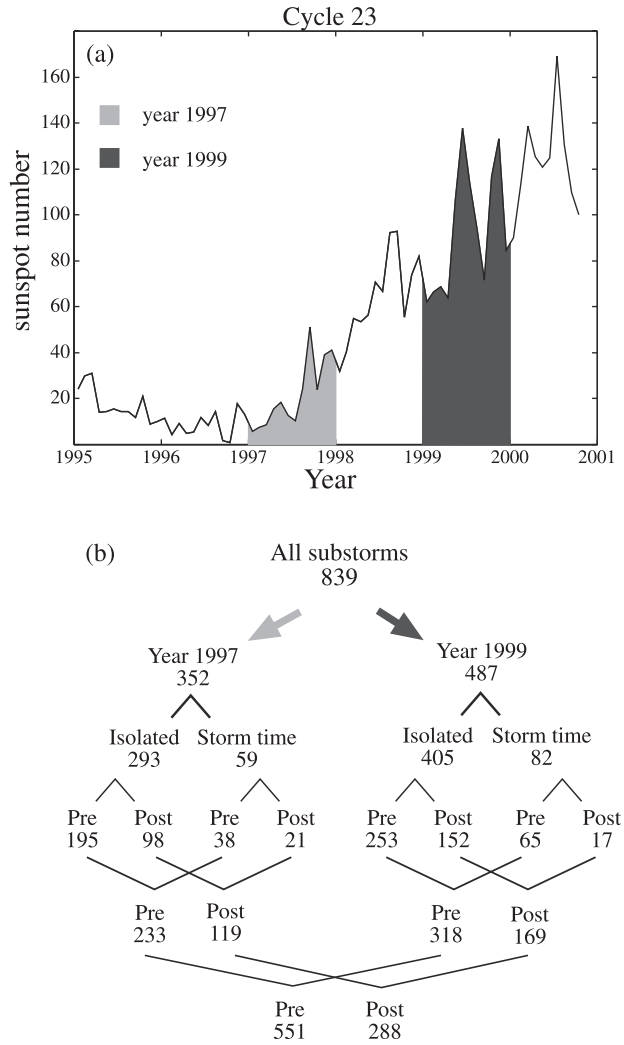

Figure 2. (a) Sunspot number during solar cycle 23. (b) Number of isolated, stormtime, premidnight, and postmidnight events during years 1997 and 1999.

3.3. Substorm Intensities and Latitudes

[23] Figures 4a and 4b show intensities, determined by the largest deviation in the north (X) component at the IMAGE magnetometers and the number of substorms in five latitudinal zones. The zones selected from south to north in geographic coordinates are as follows: (1) south of 65°, (2) 65°–69°, (3) 69°–73°, (4) 73°–76°, and (5) north of 76°. Corresponding IMAGE magnetometer array stations are (1) UPS, NUR, HAN, OUJ, LYC; (2) PEL, SOD, KIR, LOZ, MUO, ABK; (3) KIL, AND, MAS, TRO, KEV, SOR; (4) BJN; and (5) HOP, HOR, LYR, and NAL (Table 1). Substorms were assigned to the latitude bins according to the station where the maximum deviation of the X component was recorded.

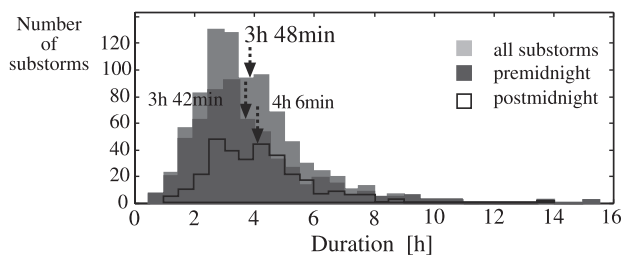

Figure 3. Substorm duration histograms for all (839), premidnight (551), and postmidnight (288) events. Histograms are binned by every 30 minutes.

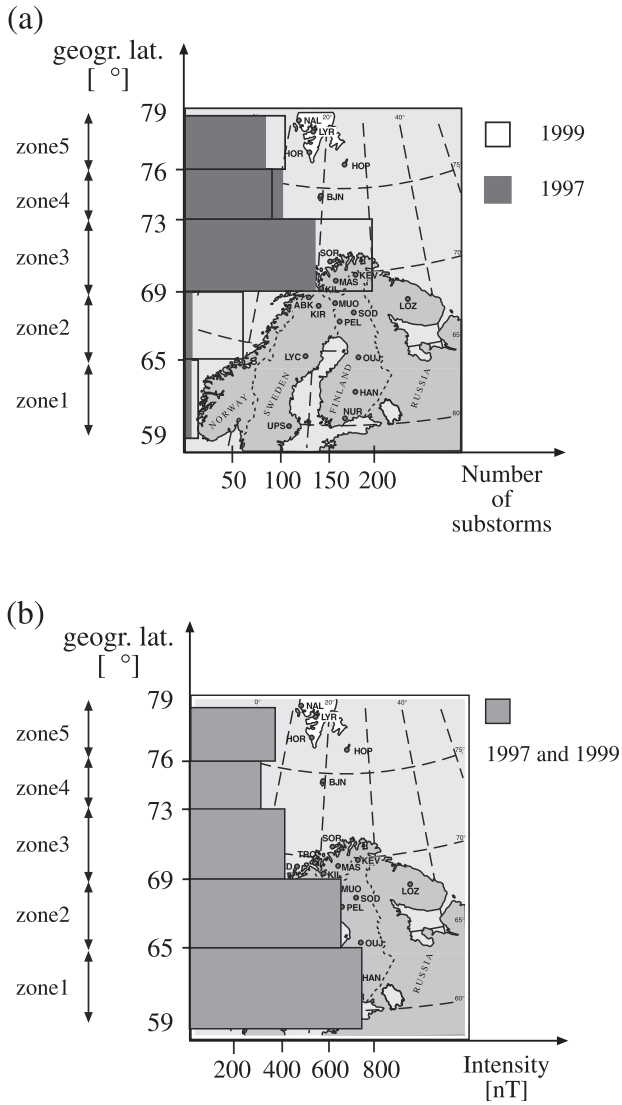

Figure 4. (a) Number of substorms in five latitudinal bins for 1997 and 1999 events, separately. The zones are selected from south to north as follows: (1) south of 65°, (2) 65°–69°, (3) 69°–73°, (4) 73°–76°, and (5) north of 76°. (b) Intensity of substorms in five latitudinal bins for 1997 and 1999. Intensities are determined by the largest deviation in the north (X) component at the IMAGE magnetometers.

[24] Figure 4a shows number of substorms in 1997 and 1999, separately. The number of the substorms maximizes in the central latitude bin, between 69°–73° in geographic latitudes (corresponding to ~66°–70° in geomagnetic latitudes), during both years. However, there are remarkably many substorms also at high latitudes, recorded by the Bear Island and Svalbard stations. In total 90% of investigated substorms recorded maximum intensity to the north of the

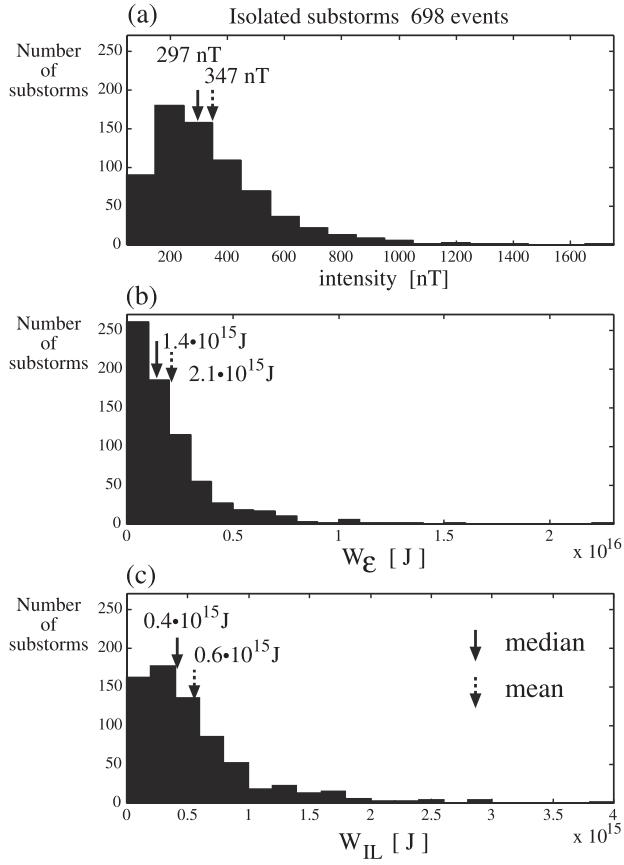

Figure 5. Intensity, energy input, and Joule dissipation histograms for 698 isolated substorms. The histograms are binned by every 100 nT in intensity, by every 10^{15} J in W_ϵ, and by every 2×10^{14} J in W_{IL}.

standard *AE* station Abisko. The large number of high-latitude substorms is a significant deficiency for the use of the standard *AE* in quantitative substorm studies, pointing out the need for longitudinally extended magnetometer chains.

[25] Figure 4b illustrates the intensity of substorms during the years 1997 and 1999. Mean intensity of substorms located in each zone was computed. On average, most intense substorms seem to be in the lowest-latitude zone, which is located south of 65°. The mean intensities for each zone from south to north are −727, −639, −407, −313, and −363 nT. Averaged maximum intensity was −418 nT for 1999 substorms and −376 nT for 1997 substorms.

4. Isolated and Stormtime Substorms

4.1. Isolated Substorms

[26] As noted above, in total, 698 isolated substorms are included in our study with the minimum intensity requirement of −100 nT in the *IL* index. Figures 5a, 5b, and 5c show intensity, energy input, and Joule dissipation histograms for isolated substorms. The entire database is binned by every 100 nT of intensity, by every 10^{15} J of W_ϵ, and by every 0.2×10^{15} J of W_{IL}. For all three quantities both mean and median values are given. The most typical intensity, in terms of the mean value, was −347 nT. Only a few isolated events were more intense than −1000 nT. Input energies varied between 0.1×10^{15} J and $10 \cdot 10^{15}$ J and the median was 1.4×10^{15} J. The median for hemispheric Joule dissipation was 0.4×10^{15} J, or roughly one third of the input energy.

[27] Joule heating dissipation, W_{IL}, as a function of solar wind energy input, W_ϵ, is plotted in Figure 6. Figure 6a shows energy input versus Joule dissipation during the substorm expansion phase, and Figure 6b shows the total

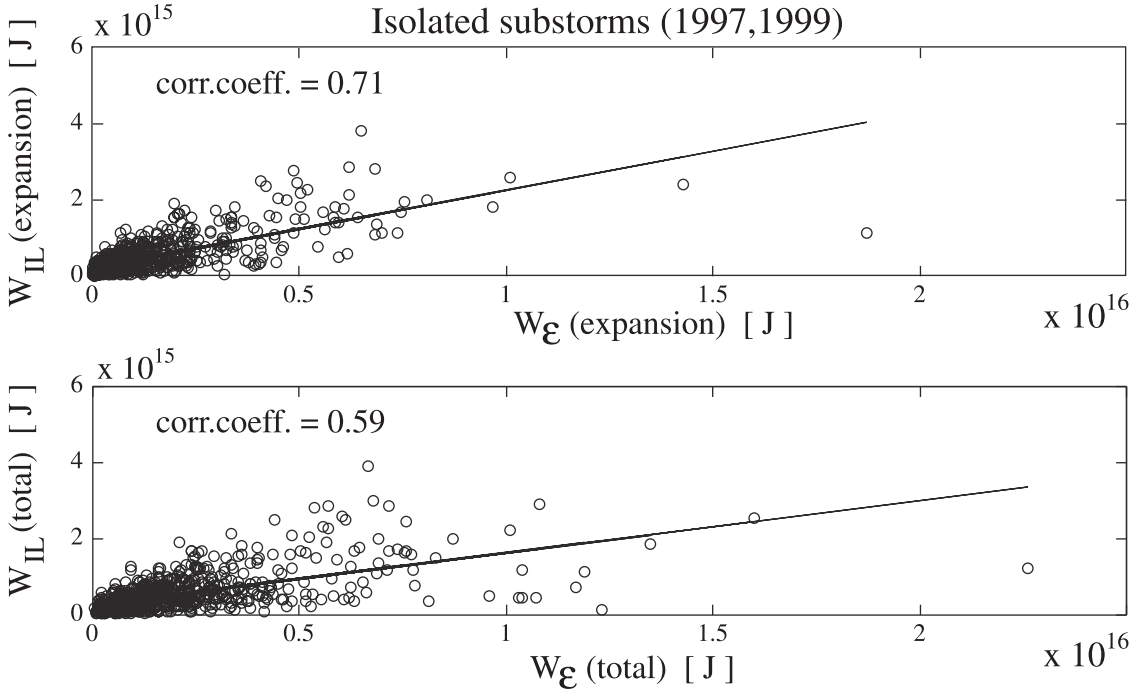

Figure 6. Joule heating dissipation, W_{IL}, for isolated substorms (1997, 1999) as a function of solar wind energy input, W_ϵ, (a) during the expansion phase and (b) during the entire substorm.

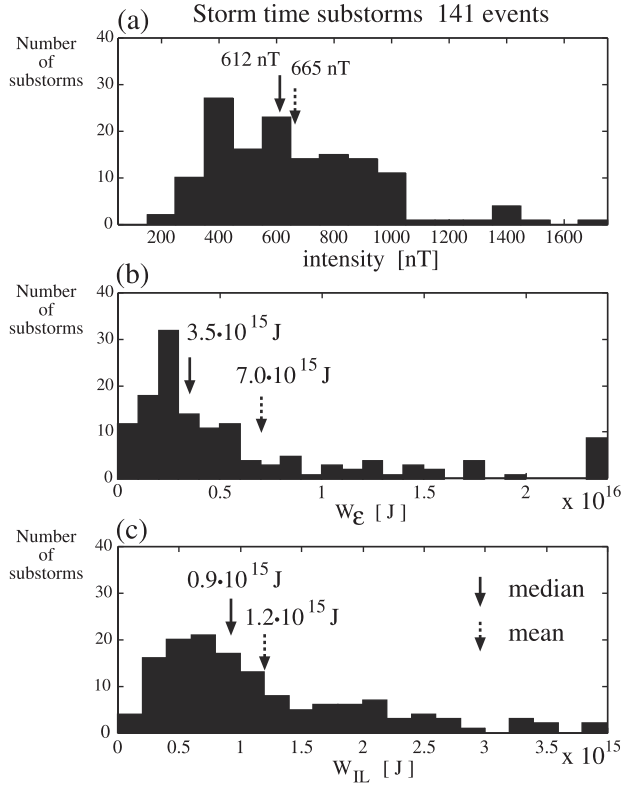

Figure 7. Intensity, energy input and Joule dissipation histograms for 141 stormtime substorms. The data are binned in the same way as in Figure 5.

energy input versus total Joule dissipation. The best correlation, 0.71, was between input and dissipation when both were evaluated during the substorm expansion phase from substorm onset to the end of the recovery phase.

4.2. Stormtime Substorms

[28] The number of the stormtime substorms, 141 events, was ~20% of the number of the isolated events, but the mean intensity of the stormtime events, −665 nT, was, as expected, much larger than the typical isolated substorm intensity. Figures 7a, 7b, and 7c show intensity, energy input, and Joule dissipation histograms for stormtime substorms in the same format as in Figure 5 (note that the scales are different). The mean energy input was 7.0×10^{15} J and the median input 3.5×10^{15} J. Large difference between the mean and the median is partly caused by large variability of stormtime solar wind conditions but may also be due to the smaller stormtime database. The median for hemispheric Joule dissipation was 0.9×10^{15} J, i.e., about one fourth of the median input.

[29] Figure 8 gives the total energy input as a function of total Joule dissipation and energy input during substorm expansion phase as a function of expansion phase Joule dissipation. The regression line is drawn from zero input to maximum energy input for isolated events, 18.7×10^{15} J. The reason for cutting the regression analysis at this level is that during very strong energy input, the ionospheric dissipation does not seem to grow with the energy input. Note that we reach the same conclusion as from Figure 6 (note again that the scales are different): the correlation coefficient between substorm expansion phase input and expansion phase output is larger than the coefficient between total input and total output. This indicates that the duration and intensity of energy dissipation during substorm expansion phase is not determined by the energy stored during the growth phase but rather by the energy that continues to be transferred to the magnetosphere during the expansion phase.

4.3. Comparison of Isolated and Stormtime Substorms

[30] As mentioned earlier, isolated substorms are five times as frequent as but half as intense as stormtime substorms. Furthermore, stormtime substorms are seldom located at latitudes higher than 73° (geographic latitude).

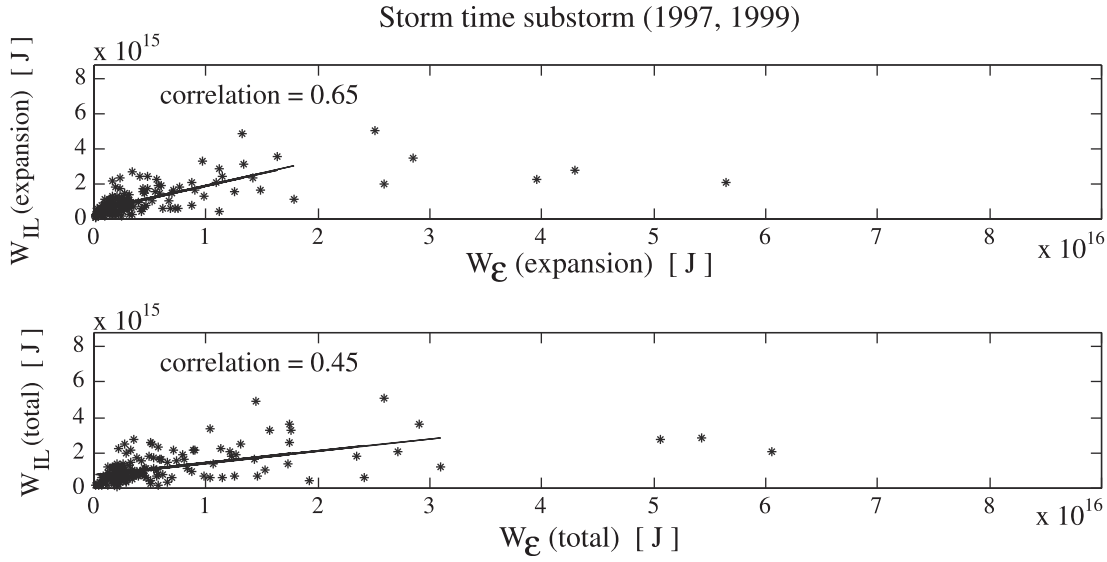

Figure 8. Joule heating dissipation for stormtime substorms (1997, 1999) as a function of solar wind energy input, separately (a) during the expansion phase and (b) during the entire substorm. Regression line is drawn, and correlation coefficient is calculated from zero to maximum energy input of isolated events, 1.87×10^{16} J.

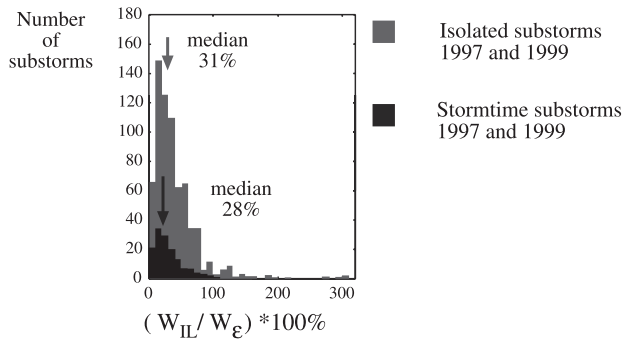

Figure 9. Ratios of W_{IL} and W_{ϵ} for isolated and stormtime events, separately.

Some larger events during storms, when the distinction between consequent substorms is more complicated and not unambiguous, cause part of the large variation in stormtime substorm energies. Comparing Figures 5b and 7b, we note that W_{ϵ} for stormtime events was ~2.5 times larger than W_{ϵ} for isolated substorms, whereas W_{IL} for stormtime events was only about two times larger than W_{IL} for isolated events. This indicates that a larger portion of W_{ϵ} is dissipated to the W_{IL} during isolated events than during stormtime events. This should hold regardless of the conversion factor between *IL* and power as long as this relationship is not too far from linear.

[31] We continued analyzing the energy input and Joule dissipation ratios by computing $(W_{IL}/W_{\epsilon}) \times 100\%$ for each event of our database. Ratios are plotted as a function of the number of substorms in Figure 9. The median for Joule heating versus energy input was 31% for isolated substorms and 28% for stormtime substorms. This indicates that during isolated events the Joule heating is more important dissipation mechanism than during stormtime substorms.

[32] Earlier in Figures 6 and 8, we showed correlations between energy input and Joule dissipation. The best correlation for isolated substorms had a correlation coefficient 0.71 (both calculated over expansion and recovery phases) and for stormtime events 0.65 (also over expansion and recovery phases). Figure 10 shows the data set further classified into premidnight and postmidnight events. The postmidnight events show even higher correlation than the full data set: 0.81 and 0.72 for isolated and stormtime events, respectively. As the auroral electrojet index *IL* specifically measures the westward current in the midnight/early morning sector, this again emphasizes the direct solar wind and IMF control of the Joule dissipation in the ionosphere.

5. Substorms During Low and High Solar Activity

[33] In this section we analyze substorms during the years 1997 and 1999 to examine substorm energy budgets during the low and the high solar activity. Active year substorms account for 58% of all events in our database. The maximum electrojet was located at lower latitudes and the substorms were slightly more intense than the quiet year events. On average, maximum intensity was −418 nT for active year substorms and −376 nT for lower activity year events.

[34] In Figure 11a we show yearly medians of energy input and Joule dissipation for both years 1997 and 1999. Figure 11a shows that the active year events, compared to the quiet year events, transferred more energy from the solar

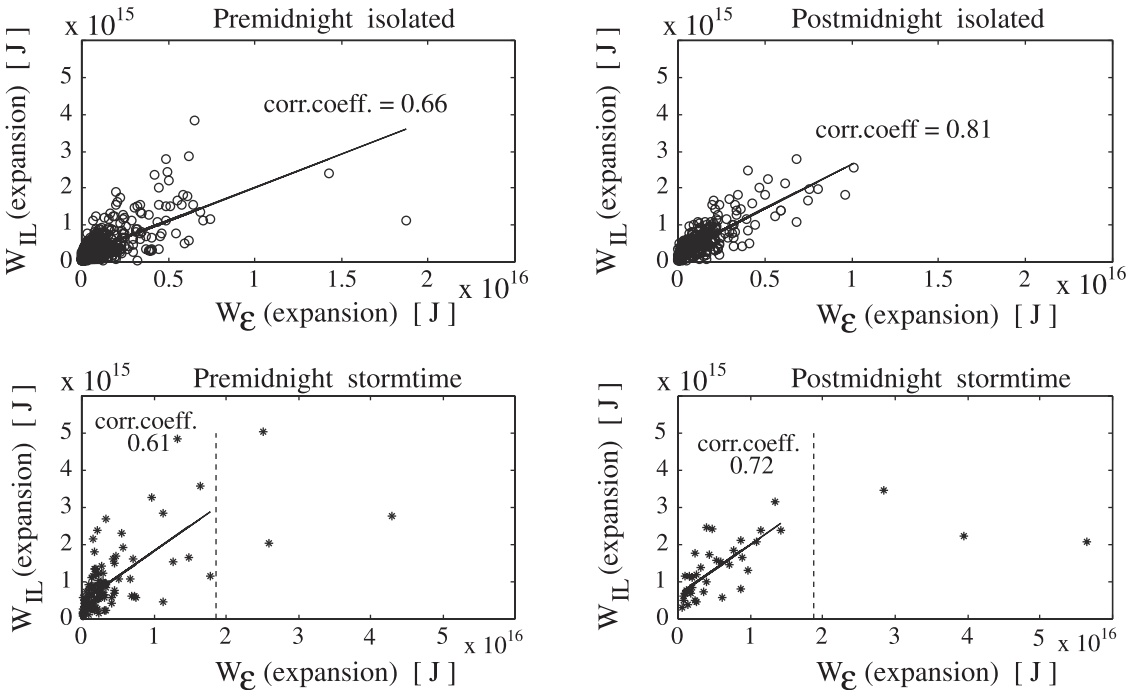

Figure 10. Joule heating during expansion phase as a function of energy input during expansion phase for (a) isolated premidnight, (b) isolated postmidnight, (c) stormtime premidnight, and (d) stormtime postmidnight events.

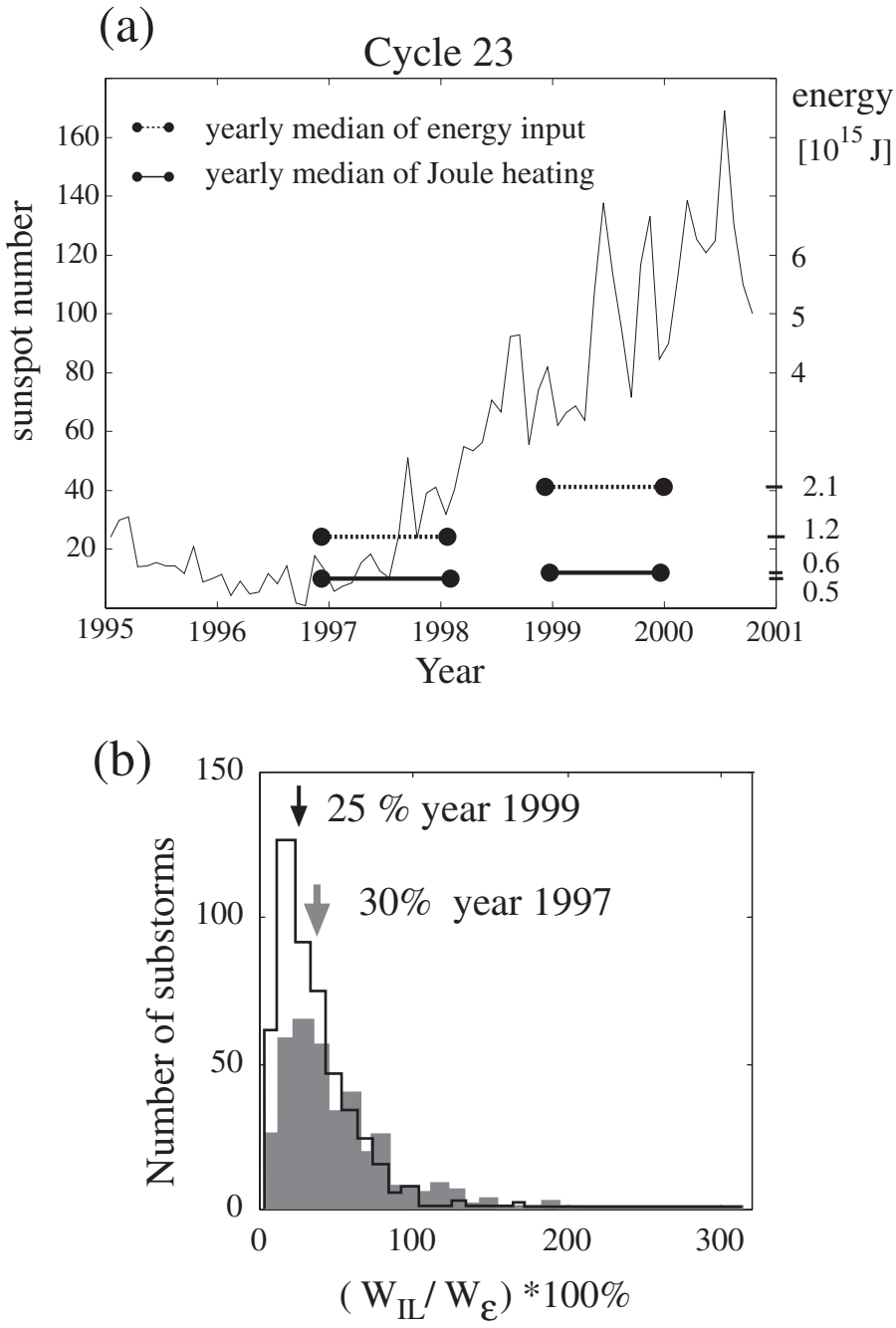

Figure 11. (a) The sunspot number and yearly averaged solar wind and Joule dissipation energies. (b) Ratios of W_{IL} and W_ϵ for 1997 (grey arrow) and 1999 (black arrow) events, separately.

wind to the magnetosphere and also dissipated more through the ionospheric Joule heating. Yearly median of energy input for lower activity solar cycle phase was 1.2×10^{15} J and for higher activity phase 2.1×10^{15} J. Annually averaged Joule heating was slightly larger for the more active solar cycle phase.

[35] Substorm energy budget was studied by comparing the Joule heating to the total energy input. In Figure 11b the number of substorms is plotted as a function of $(W_{IL}/W_\epsilon) \times 100\%$ binned by every 10%. Same kind of curve is plotted for substorms of both years 1997 and 1999. Median of ratios of W_{IL} and W_ϵ are marked with arrows. The Northern Hemisphere Joule heating dissipates about one third (30%) of solar wind energy input during 1997 and about one fourth (25%) during 1999. If the two-hemisphere Joule heating would be twice the Northern Hemisphere Joule heating then global Joule heating would cover ~60% of total energy input, on average. That clearly shows that Joule heating dominates over the other dissipation channels during substorms. Note that substorms with $W_{IL} > 0.5\ W_\epsilon$ are

events of very small input when the substorms most likely unloaded previously stored energy (cf. scatterplots in Figures 6 and 8).

6. Discussion

[36] The relative role of ionospheric Joule heating in the global magnetospheric energy budget is an important issue. When *Perreault and Akasofu* [1978] derived the epsilon parameter, it was generally believed that ~90% of energy dissipation would be through ring current injection, but this value has been gradually changing [*Weiss et al.*, 1992; *Knipp et al.*, 1998]. The recent results of Turner et al. (submitted manuscript, 2001) show that Joule heating actually dominates over the ring current as a dissipation channel, even during storm events. They estimate that Joule heating accounts for ~50% or more of the stormtime energy dissipation whereas the ring current accounts only for 10%–15%. We found that for substorms studied in this paper the Northern Hemisphere Joule heating accounted for about one third in 1997 and about one fourth in 1999. Thus, during the quiet year, Joule dissipation appears to cover a larger part of energy budget than during the active year, when the ring current may be a more efficient dissipation channel. The global Joule heating over both hemispheres is likely to be approximately twice the Northern Hemisphere heating, but owing to lack of observations in the Southern Hemisphere, we consider one-hemisphere values only.

[37] It is important to note that the methods in evaluating the energy output in the works of *Knipp et al.* [1998], Turner et al. (submitted manuscript, 2001) and in this study are different, but all studies use the same epsilon parameter as input. Thus the increased relative role of the ionospheric dissipation as compared to the estimates in the early 1980s is a consistent conclusion. There is still the possibility that the tail dissipation is underestimated, and if so, the scaling of epsilon, i.e., the parameter l_0, may need revision.

[38] An interesting question is whether changing solar activity is related to changes in substorm activity [e.g., *King*, 1979; *Slavin et al.*, 1986]. The annually averaged Joule dissipation was only 0.1×10^{15} J larger in 1999 than in 1997 (Figure 11a), which may not be statistically significant considering the uncertainties in the procedure to derive the Joule heating rate from magnetometer observations. Note, however, that in 1999, there were 38% more events, they were 11% more intense, on average, and they were located at lower latitudes than during the year 1997. It would be useful to redo this study in the future during the descending solar cycle when the high-speed streams begin to arrive, as was also suggested by *Holzer and Slavin* [1981].

[39] Isolated and stormtime substorms studied in this paper showed some different characteristics. The intensities of stormtime substorms were twice the intensities of isolated substorms. Our results agree with *Hsu and McPherron* [2000], who showed that in terms of absolute values and changes of magnitude, the stormtime substorms are larger than isolated substorms. Additionally, stormtime substorms that we studied carried more energy from solar wind to the ionospheric Joule heating than the isolated ones: On average, Northern Hemisphere Joule dissipation for stormtime substorms was 0.9×10^{15} J and for isolated substorms about half of that. Dividing the typical stormtime Joule dissipation energy, 0.92×10^{15} J, by the typical substorm duration, 3 hours 48 min, we end up with a characteristic value of a Northern Hemisphere stormtime substorm of 62 GW. Considering the large uncertainties in these numbers and the large variations from event to event, the result is consistent with an AMIE event study result [*Lu et al.*, 1998], which gives an average power of 190 GW over both hemispheres during a 2-day magnetic cloud event. Note that the AMIE calculation was made without taking into account the effect of the neutral wind, which tends to reduce the Joule dissipation by ~30% [*Lu et al.*, 1995].

[40] The solar wind-magnetosphere interaction includes both directly driven and loading-unloading processes [*Baker et al.*, 1984; *Bargatze et al.*, 1985]. Substorm energy within the context of the near-Earth neutral line (NENL) model comes from reconnection at the dayside magnetopause transferring magnetic flux to the tail where it is eventually dissipated and returned by reconnection at the NENL. If dayside reconnection ceases near or just after the onset of the expansion phase, then the substorm is said to have resulted from an ''unloading'' of the energy stored in the tail lobes during the growth phase. Alternatively, if much or most of the energy powering the substorm comes from the reconnection of newly arrived flux tubes during the expansion phase, then the substorm is said to be ''directly driven.''. Our results indicate that while there is no doubt that stored energy is dissipated during substorms [e.g., *Caan et al.*, 1975], the energy transferred to the magnetosphere during the expansion phase is clearly more significant than the dissipation of the stored energy.

[41] In our previous paper [*Kallio et al.*, 2000] we showed that the size of the substorm is mostly governed by the direct energy input during the expansion phase if the energy input does not cease soon after the growth phase. Results of the present study show that the strongest correlation, 0.81, between energy input from the solar wind and Joule heating dissipation was obtained for isolated, postmidnight substorm events when the energy input and output during expansion phase only were taken into account. As the directly driven convection electroject, beginning in this sector, dominate over the substorm electrojet, this new result further emphasizes the interpretation that the direct energy input plays an essential role in substorm dynamics during the substorm expansion phase, whereas the energy loaded during the growth phase is more important for the processes related to the substorm onset.

7. Summary of Results

[42] Differences between the active year (1999) and the quiet year (1997) are the following:

1. Northern Hemisphere Joule heating accounts for about one third of solar wind energy input during 1997 and about one fourth during 1999.
2. In 1999, there were more events, and they were at lower latitudes than in 1997.
3. Averaged maximum intensity was −418 nT for 1999 substorms and −376 nT for 1997 substorms.

[43] The key results for the entire statistics are the following:

1. The Northern Hemisphere Joule heating accounts for ~30% of solar wind energy input.

2. While the energy loaded during the growth phase is necessary for the magnetospheric reconfiguration before the substorm onset (the growth phase energy is never zero), the size of the substorm as measured by the *IL* index is mostly governed by the direct energy input during the expansion phase.

3. The strongest correlation, 0.81, between energy input and Joule dissipation was found during the expansion phase of isolated substorms in postmidnight sector. This indicates that the directly driven processes are important for determining the size of the substorms as measured by ionospheric electrojet indices.

4. Isolated substorms are five times as frequent as, but only half as intense as, stormtime substorms. However, during isolated substorms the Joule heating was more important dissipation mechanism than during storms.

5. Nine substorm events out of ten have their maximum *IL* intensity at higher latitudes than the standard *AE* station Abisko. This suggests that the standard index misses or underestimates portion of substorm events.

[44] **Acknowledgments.** We wish to thank R. Lepping for the Wind magnetic field data, A. Lazarus for the Wind solar wind data, C. Smith for the ACE magnetic field data, D. McComas for the ACE solar wind data, and all the institutes maintaining the IMAGE magnetometer network. Wind and ACE data were obtained through CDAWeb. The work of E.T. was supported by the Academy of Finland.

[45] Michel Blanc thanks the two referees for their assistance in evaluating this paper.

References

Ahn, B.-H., S.-I. Akasofu, and Y. Kamide, The Joule heat production rate and the particle energy injection rate as a function of the geomagnetic indices AE and AL, *J. Geophys. Res.*, *88*, 6275, 1983.

Akasofu, S.-I., Energy coupling between the solar wind and the magnetosphere, *Space Sci. Rev.*, *28*, 121, 1981.

Baker, D. N., Solar wind-magnetosphere drivers of space weather, *J. Atmos. Terr. Phys.*, *58*, 14, 1996.

Baker, D. N., S.-I. Akasofu, W. Baumjohann, J. W. Bieber, D. H. Fairfield, E. W. Hones Jr., B. Mauk, R. L. McPherron, and T. E. Moore, Substorms in the magnetosphere, in *Solar Terrestrial Physics - Present and Future*, *NASA Publ.*, *1120*, 1984.

Bargatze, L. F., D. N. Baker, R. L. McPherron, and E. W. Hones Jr., Magnetospheric impulse response for many levels of geomagnetic activity, *J. Geophys. Res.*, *90*, 6387, 1985.

Baumjohann, W., Y. Kamide, and R. Nakamura, Substorms, storms, and the near-Earth tail, *J. Geomagn. Geoelectr.*, *48*, 177, 1996.

Caan, M. N., R. L. McPherron, and C. T. Russell, Substorm and interplanetary magnetic field effects on the geomagnetic tail lobes, *J. Geophys. Res.*, *80*, 191, 1975.

Cowley, S. W. H., and M. Lockwood, Excitation and decay of solar wind-driven flows in the magnetosphere-ionosphere system, *Ann. Geophys.*, *10*, 103, 1992.

Davis, T. N., and M. Sugiura, Auroral electrojet activity index AE and its universal time variations, *J. Geophys. Res.*, *71*, 785, 1966.

Holzer, R. E., and J. A. Slavin, The effect of solar wind structure on magnetospheric energy supply during solar cycle 20, *J. Geophys. Res.*, *86*, 675, 1981.

Holzer, R. E., and J. A. Slavin, An evaluation of three predictors of geomagnetic activity, *J. Geophys. Res.*, *87*, 2558, 1982.

Hones, E. W., Jr., et al., Structure of the magnetotail at 220 R_E and its response to geomagnetic activity, *Geophys. Res. Lett.*, *11*, 5, 1984.

Hsu, T.-S., and R. L. McPherron, The characteristics of storm-time substorms and non-storm substorms, Proceedings of the International Conference on Substorms (ICS-5), *Eur. Space Agency, Spec. Publ., ESA SP-443*, 439, 2000.

Ieda, A., S. Machida, T. Mukai, Y. Saito, T. Yamamoto, A. Nishida, T. Terasawa, and S. Kokobun, Statistical analysis on the plasmoid evolution with Geotail observations, *J. Geophys. Res.*, *103*, 4453, 1998.

Kallio, E. I., T. I. Pulkkinen, H. E. J. Koskinen, A. T. Viljanen, J. A. Slavin, and K. Ogilvie, Loading-unloading processes in the nightside ionosphere, *Geophys. Res. Lett.*, *27*, 627, 2000.

Kamide, Y., et al., Current understanding of magnetic storms: Storm-substorm relationship, *J. Geophys. Res.*, *21*, 17,705, 1998.

Kauristie, K., T. I. Pulkkinen, R. J. Pellinen, and H. J. Opgenoorth, What can we tell about auroral electrojet activity from a single meridional magnetometer chain, *Ann. Geophys.*, *14*, 1177, 1996.

King, J. H., Solar cycle variations in IMF intensity, *J. Geophys. Res.*, *84*, 5938, 1979.

Knipp, D. J., et al., An overview of the early November 1993 geomagnetic storm, *J. Geophys. Res.*, *103*, 26,197, 1998.

Lepping, R. P., et al., The Wind magnetic field investigation, *Space Sci. Rev.*, *71*, 207, 1995.

Lu, G., D. Richmond, B. A. Emery, and R. G. Roble, Magnetosphere-ionosphere-thermosphere coupling: Effect of neutral winds on energy transfer and fild-aligned current, *J. Geophys. Res.*, *100*, 19,643, 1995.

Lu, G., et al., Global energy deposition during the January 1997 magnetic cloud event, *J. Geophys. Res.*, *103*, 11,685, 1998.

McComas, D. J., S. J. Bame, P. Barker, W. C. Feldman, J. L. Phillips, P. Riley, and J. W. Griffee, Solar wind electron proton alpha monitor (SWEPAM) for the advanced composition explorer, *Space Sci. Rev.*, *86*, 563, 1998.

McPherron, R. L., C. T. Russell, and M. P. Aubry, Satellite studies of magnetospheric substorms on August 15, 1968, 9, Phenomenological models for substorms, *J. Geophys. Res.*, *78*, 3131, 1973.

Moldwin, M. B., and W. J. Hughes, Geomagnetic substorm association of plasmoids, *J. Geophys. Res.*, *98*, 81, 1993.

Ogilvie, K. W., D. J. Chornay, R. J. Fritzenreiter, F. Hunsaker, J. Keller, J. Lobell, G. Miller, J. D. Scudder, and E. C. Sittler, Jr., SWE, A Comprehensive plasma instrument for the WIND spacecraft, *Space Sci. Rev.*, *71*, 55, 1995.

Perreault, P., and S.-I. Akasofu, A study of geomagnetic storms, *Geophys. J. R. Astr. Soc.*, *54*, 547, 1978.

Petrukovich, A. A., E. I. Kallio, T. I. Pulkkinen, and H. E. J. Koskinen, Solar wind energy input and magnetospheric substorm activity compared, Proceedings of ICS-5, *Eur. Space Agency, Spec. Publ., ESA SP-443*, 67, 2000.

Pulkkinen, T. I., N. Y. Ganushkina, E. I. Kallio, G. Lu, D. N. Baker, N. E. Turner, T. A. Fritz, J. F. Fennell, and J. Roeder, Energy dissipation during a geomagnetic storm: May 1998, *Adv. Space Res.*, in press, 2002.

Ridley, A. J., G. Lu, C. R. Clauer, and V. O. Papitashvili, Ionospheric convection during nonsteady interplanetary conditions, *J. Geophys. Res.*, *102*, 14,564, 1997.

Ridley, A. J., G. Lu, C. R. Clauer, and V. O. Papitashvili, A statistical study of the ionospheric convection response to changing interplanetary conditions using the assimilative mapping of ionospheric electrodynamics technique, *J. Geophys. Res.*, *103*, 4023, 1998.

Rostoker, G., S.-I. Akasofu, J. Foster, R. A. Greenwald, Y. Kamide, K. Kawasaki, A. T. Y. Lui, R. L. McPherron, and C. T. Russell, Magnetospheric substorms—Definition and signatures, *J. Geophys. Res.*, *85*, 1663, 1980.

Rostoker, G., J. C. Samson, F. Creutzberg, T. J. Hughes, D. R. McDiarmid, A. G. McNamara, A. Vallance Jones, D. D. Wallis, and L. L. Cogger, CANOPUS: A groundbased instrument array for remote sensing the high latitude ionosphere during the ISTP/GGS program, *Space Sci. Rev.*, *71*, 743, 1995.

Ruohoniemi, J. M., and R. A. Greenwald, The response of high-latitude convection to a sudden southward IMF turning, *Geophys. Res. Lett.*, *25*, 2913, 1998.

Russell, C. T., and R. L. McPherron, Semiannual variation of geomagnetic activity, *J. Geophys. Res.*, *78*, 92, 1973.

Slavin, J. A., G. Jungman, and E. J. Smith, The interplanetary magnetic field during solar cycle 21: ISEE-3/ICE observations, *Geophys. Res. Lett.*, *13*, 513, 1986.

Smith, C. W., J. L'Heureux, N. F. Ness, M. H. Acuna, L. F. Burlaga, and J. Scheifele, The ACE magnetic fields experiments, *Space Sci. Rev.*, *86*, 613, 1998.

Stamper, R., M. Lockwood, M. N. Wild, and T. D. G. Clark, Solar causes of the long-term increase in geomagnetic activity, *J. Geophys. Res.*, *104*, 28,325, 1999.

Syrjäsuo, M., et al., Observations of substorm electrodynamics using the MIRACLE network, in *Substorms-4*, edited by S. Kokubun and Y. Kamide, pp. 111–114, Terra Sci., Tokyo, 1998.

Weiss, L. A., P. H. Reiff, J. J. Moses, R. A. Heelis and B. D. Moore, Energy dissipation in substorms, *Proceedings of the International Conference on Substorms (ICS-1)*, *Eur. Space Agency, Spec. Publ., ESA SP-335*, 309, 1992.

H. E. J. Koskinen, T. I. Pulkkinen, and E. Tanskanen, Geological Research, Finnish Meteorological Institute, P.O. Box 503, FIN-00101, Helsinki, Finland.

J. A. Slavin, NASA Goddard Space Flight Center, Greenbelt, MD 20771, USA.